

## Domain boundaries in the GaAs(001)-2×4 surface

M. Takahasi,<sup>1</sup> Y. Yoneda,<sup>1</sup> N. Yamamoto,<sup>2</sup> and J. Mizuki<sup>1,2</sup>

<sup>1</sup>Synchrotron Radiation Research Center, Japan Atomic Energy Research Institute, Mikazuki-cho, Hyogo 679-5148, Japan

<sup>2</sup>Faculty of Science, Himeji Institute of Technology, Kamigori-cho, Hyogo 678-1297, Japan

(Received 16 November 2002; revised manuscript received 24 June 2003; published 21 August 2003)

The  $\alpha$ ,  $\beta$ , and  $\gamma$  phases of the GaAs(001)-2×4 surface have been investigated by *in situ* surface x-ray diffraction in an As flux and at temperatures ranging from 480 °C to 610 °C. It has been found that the fractional-order peaks originating from the fourfold symmetry show shift in the [110] direction as well as significant broadening of the peaks in the  $\alpha$  and  $\gamma$  phases. The direction of the peak shift is characteristic in each phase. This behavior is explained by the formation of the antiphase domain boundaries. The atomic structure of the domain boundaries is discussed.

DOI: 10.1103/PhysRevB.68.085321

PACS number(s): 68.35.Bs, 61.10.-i, 81.05.Ea

The GaAs(001) surface is the most widely used surface in the molecular-beam-epitaxy (MBE) growth of the III-V group semiconductor devices. Under growth conditions, the GaAs(001) surface is exposed to the gas phase of source materials and thus exchanges atoms with the environment. Hence, a variety of surface compositions different from the bulk stoichiometry are allowed at the surface, depending on temperature and the partial pressure of As. Through a number of experiments, a series of reconstructions including  $c(4\times 4)$ ,  $2\times 4$ ,  $2\times 6/3\times 6$ , and  $c(8\times 2)$  has been identified. The most important of these reconstructions is the As-stabilized  $2\times 4$  surface, since it is observed in the optimum condition for homoepitaxial growth of GaAs(001). On the basis of a reflection high-energy electron-diffraction (RHEED) study, the  $2\times 4$  structure has been subdivided into the  $\alpha$ ,  $\beta$ , and  $\gamma$  phases, which are distinguishable by the relative intensities of the fractional-order streaks along the [110] direction.<sup>1</sup> The diffraction features of RHEED were analyzed using kinematical calculation, and attributed to the difference in atomic arrangement within the  $2\times 4$  unit cell.<sup>1</sup> The  $\alpha$ ,  $\beta$ , and  $\gamma$  phases were assigned to the  $\alpha$ -( $2\times 4$ ) structure with an As coverage of 0.5 ML (monolayer), the  $\beta$ -( $2\times 4$ ) structure with an As coverage of 0.75 ML, and the  $\gamma$ -( $2\times 4$ ) structure with an As coverage of 1.0 ML, respectively. The three phases of the ( $2\times 4$ ) surface have been recognized also by reflectance-difference spectroscopy (RDS).<sup>2,3</sup>

However, recent work suggests that the  $\alpha$ ,  $\beta$ , and  $\gamma$  phases are basically the same structure. Scanning tunneling microscopy (STM) has shown that the outermost surface layer consists of two As dimers and two As vacancies in these three phases.<sup>4-6</sup> Moreover, the dynamical analysis of RHEED rocking curves revealed similarity among the  $\alpha$ ,  $\beta$ , and  $\gamma$  phases.<sup>7</sup> For the  $\beta$  phase, the  $\beta 2$ -( $2\times 4$ ) structure, which differs from the  $\beta$ -( $2\times 4$ ) structure in the number of As dimers in the first layer, has been established both experimentally<sup>4,5,8,9</sup> and theoretically.<sup>10-13</sup> Thus it is likely that the  $\alpha$ ,  $\beta$ , and  $\gamma$  phases have the  $\beta 2$ -( $2\times 4$ ) structure in common. The major difference among the  $\alpha$ ,  $\beta$ , and  $\gamma$  phases is the density of defects. A high degree of disorder has been found in the  $\alpha$  and  $\gamma$  phases whereas the long-range order extends over 1000 Å in the  $\beta$  phase.<sup>4,5,14-20</sup> In the  $\gamma$

phase, the disorder was explained by the effect of excess As incorporated into the  $\beta 2$ -( $2\times 4$ ) structure<sup>5,16</sup> or coexistence of the  $\beta 2$ -( $2\times 4$ ) and  $c(4\times 4)$  structures.<sup>4,19,20</sup> It was shown, in the  $\alpha$  phase, that the disorder is caused by spontaneous island formation.<sup>17,18</sup>

In this paper, we focus on the long-range feature of the disorder in the  $\alpha$  and  $\gamma$  phases, which was less discussed in previous atomic-scale studies using STM. We carried out *in situ* x-ray measurements under MBE conditions, while existing STM studies were performed at room temperature for quenched samples. X-ray results show that there is a distinctive tendency in the disorder observed in the  $\alpha$  and  $\gamma$  phases. In the  $\alpha$  and  $\gamma$  phases, the  $2\times 4$  domains are separated by the antiphase domain boundary which is characteristic to each phase. The preference in the antiphase domain boundary can be explained by the structure model where another metastable reconstruction is formed between the  $\beta 2$ -( $2\times 4$ ) domains. This model brings about a detailed understanding of the phase transition between the reconstructions on the GaAs(001) surface.

The experiments were performed on the synchrotron-radiation beamline 11XU at SPring-8, Japan, using a surface x-ray diffractometer.<sup>21</sup> This diffractometer is directly coupled to an MBE chamber equipped with RHEED and five Knudsen cells so as to allow *in situ* x-ray measurements during growth.

The sample was cut to  $15\times 15\times 0.3$  mm<sup>3</sup> from an on-axis GaAs(001) wafer doped with Si ( $2\times 10^{17}$  cm<sup>-3</sup>), mounted on a molybdenum block with indium and transferred to the MBE chamber. After removal of the oxide at 580 °C, buffer layers of 0.2  $\mu$ m thickness were grown at a rate of 0.1  $\mu$ m/h at a substrate temperature of 550 °C and an As pressure of  $10^{-6}$  Torr. The As pressure was kept at  $5\times 10^{-7}$  Torr during the x-ray measurements.

The x-ray wavelength used was 1.24 Å. The resolution in the reciprocal-lattice space was determined by the receiving slit in front of the detector to be  $5\times 10^{-4}$  Å<sup>-1</sup> in the transverse direction and  $3\times 10^{-2}$  Å<sup>-1</sup> in the radial direction. In the present paper, the reflections ( $H, K, L$ ) are described on the basis of a surface  $1\times 1$  unit cell which is defined by  $\mathbf{a} = a_0/\sqrt{2}(1, -1, 0)_{\text{cubic}}$ ,  $\mathbf{b} = a_0/\sqrt{2}(1, 1, 0)_{\text{cubic}}$  in the surface plane, and  $\mathbf{c} = a_0(0, 0, 1)_{\text{cubic}}$  in the surface normal direction with the lattice constant of GaAs,  $a_0$ .

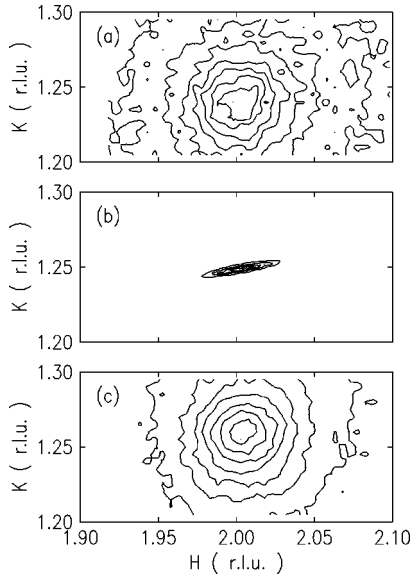


FIG. 1. Intensity distribution of x rays around (2,1.25,0.04) in the  $HK$  plane. (a) The  $\alpha$  phase at a substrate temperature of 610 °C. (b) The  $\beta$  phase at 520 °C. (c) The  $\gamma$  phase at 480 °C.

Figure 1 shows the distribution of the x-ray-diffraction intensity around (2, 1.25, 0.04), which arises from fourfold symmetry along the [110] direction. The RHEED showed  $\alpha$ ,  $\beta$ , and  $\gamma$  patterns at temperatures of 610 °C, 520 °C, and 480 °C, respectively. While a sharp x-ray diffraction peak occurs at (2,1.25,0.04) in the  $\beta$  phase, a broad peak indicative of disorder is observed in the  $\alpha$  and  $\gamma$  phases. The peak broadens isotropically. More importantly, it was found that the peak position shifts along the  $K$  direction while it remains at  $H=2$ . The peak occurs at  $K$  slightly less than 1.25 in the  $\alpha$  phase and at  $K$  larger than 1.25 in the  $\gamma$  phase.

The direction of the peak shift also depends on the reflection index. Figure 2 shows the peak profiles along  $K$  for different reflections in the  $\alpha$ ,  $\beta$ , and  $\gamma$  phases. The measurement temperatures are 605 °C, 520 °C, and 480 °C, respectively. As already shown in Fig. 1, the peak (2,1.25,0.04) moves to  $K$  smaller than 1.25 in the  $\alpha$  phase and in the opposite direction in the  $\gamma$  phase. However, the direction of the shift is inverted for the peak at (2,0.75,0.04). In the  $\alpha$  phase, the peak position is larger than  $K=0.75$  while it is smaller than  $K=0.75$  in the  $\gamma$  phase. In contrast to these two peaks, the peak at (2,0.5,0.04) remains at  $K=0.5$  even in the  $\alpha$  and  $\gamma$  phases, although it becomes as broad as other reflections. No significant shift of the peak was observed for the integral-order peak (2,1,0.04) at these temperatures. Thus, this behavior is summarized as the following: the peaks at  $K=(4m\pm 1)/4$  ( $m$  is an integral number) move so as to approach the integral-order peaks in the  $\alpha$  phase, while the direction of the peak shift is inverted in the  $\gamma$  phase.

The observed peak shifts result from the evolution of antiphase boundaries among the  $2\times 4$  domains because they are accompanied by broadening of the fractional-order peaks. In general, the antiphase domain boundaries may be caused by steps. In this case, the antiphase should broaden the integral-order peaks as well as the fractional-order peaks,

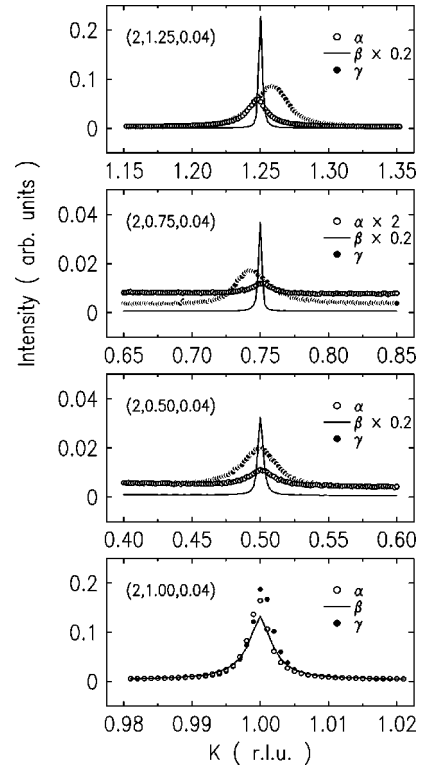


FIG. 2. Peak profiles of different reflections in the  $\alpha$ ,  $\beta$ , and  $\gamma$  phases.

since the domains shift by half of the lattice constant  $a$  at 1 ML-high steps. However, the peak at (2,1.00,0.04) was keeping a similar profile through the  $\alpha$ ,  $\beta$ , and  $\gamma$  phases as shown in Fig. 2. This shows that the antiphase domain boundaries occur within a terrace and that the shift of the domains is given by  $na$  with an integer  $n$ . Thus, the formation of steps has a minor effect on the change of the fractional-order peaks.

In order to explain the observed peak shifts, we introduce a simple one-dimensional model. Suppose there is a system consisting of an array of  $M$  scatterers in the [110] direction. The spacing between the scatterers is assumed to have a value of  $na$  by the probability  $p_n$ , with the  $1\times 1$  lattice constant  $a=a_0/\sqrt{2}$ . For the perfect arrangement of scatterers with a period  $4a$ , the probability  $p_4$  is unity and the others are zero. If the system includes the antiphase domain boundaries, the spacings of the scatterers are different from  $4a$  according to the distribution of  $p_n$ . The amplitude of the diffracted wave from the whole system is the coherent sum of the contribution from all the scatterers. Thus the diffracted intensity is given by

$$I = M|f|^2 + \sum_{k \neq k'} |f|^2 \exp[2\pi i q(R_k - R_{k'})], \quad (1)$$

where  $q$  is the relevant component of the scattering vector,  $R_k$  is the position of the scatterer  $k$ , and  $f$  is the scattering factor of a single scatterer. To calculate the averaged diffracted intensity, we introduce the averaged phase difference between the  $l$ th nearest neighbor  $\Phi_l$ , which is defined by

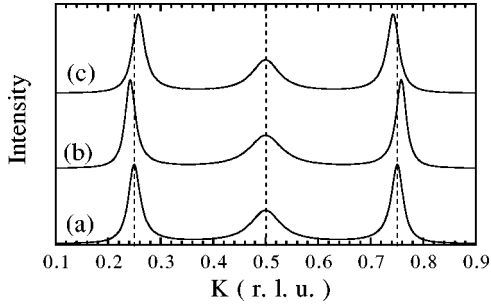


FIG. 3. Simulation of the diffracted intensity for (a)  $p_3=p_5=0.14$ , (b)  $p_3=0.07, p_5=0.21$ , and (c)  $p_3=0.21, p_5=0.07$ . For all the cases,  $p_4$  was fixed to be 0.72.

$$\Phi_l = \left[ \sum_n p_n \exp(2\pi i q n a) \right]^l. \quad (2)$$

Considering that the number of the  $l$ th nearest neighbor is  $M-l$ , the averaged diffracted intensity is calculated as the following:

$$I = M|f|^2 + 2|f|^2 \text{Re} \sum_{l=1}^M (M-l)\Phi_l. \quad (3)$$

For  $M \rightarrow \infty$ , the normalized intensity is given by

$$\frac{I}{M} = |f|^2 \left( 1 + 2 \text{Re} \left[ \frac{\Phi_1}{1-\Phi_1} \right] \right). \quad (4)$$

First, we show that this one-dimensional model accounts for the observed shift of the diffraction peaks qualitatively. In Fig. 3, a comparison is made for different  $p_3$  and  $p_5$  while  $p_4$  is kept as 0.72. The abscissa are expressed in terms of the reciprocal-lattice unit,  $K=qa$ . For  $p_3=p_5=0.14$ , the diffracted intensity is calculated as curve (a). Although the peaks have a finite width due to the presence of the antiphase domain boundaries, they occur at exactly quarter-order points of  $K$ . When either  $p_3$  or  $p_5$  is dominant, however, the peaks at  $K=0.25$  and  $K=0.75$  slightly move from the original positions. For  $p_3=0.07$  and  $p_5=0.21$ , the peaks move so as to move away from  $K=0.5$ . This is the case of the  $\alpha$  phase. In contrast, the peaks approach  $K=0.5$  for  $p_3=0.21$  and  $p_5=0.07$ , corresponding to the  $\gamma$  phase. This simulation leads us to the conclusion that the  $\alpha$  and  $\gamma$  phases are related to the antiphase domain boundary characteristic to each phase. It is shown by further simulation that the antiphase domain boundaries with  $n=(4m-1)$  and  $n=(4m+1)$  work equivalently to  $n=3$  and  $n=5$ , respectively, with respect to the peak shifts.

The distribution of  $p_n$  can be evaluated by the fitting with this model. The solid lines in Fig. 4 show the results of the fitting for the peaks at  $K=1.25$  in the  $\alpha$  and  $\gamma$  phases. A restriction is applied to the fitting parameters so that  $\sum_n p_n = 1$ . To obtain a reasonable fitting to all the measured peaks at  $K=0.5, 0.75$ , and  $1.25$ , the inclusion of  $p_6$  in addition to  $p_3$  and  $p_5$  was necessary. For the  $\gamma$  phase, the optimized parameters are  $p_3=0.14(1)$ ,  $p_4=0.79(1)$ ,  $p_5=0.01(1)$ , and  $p_6=0.06(1)$ . The domain boundary of  $n=4m-1$  is domi-

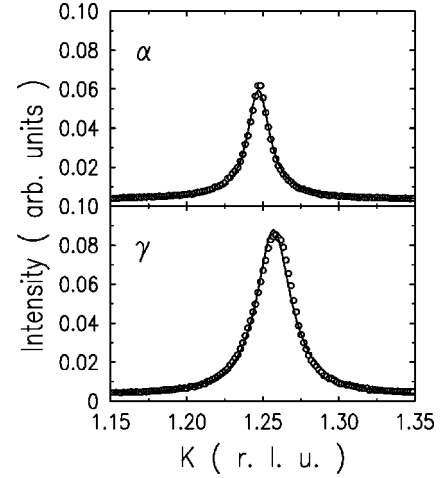


FIG. 4. Result of the fitting for the  $\alpha$  and  $\gamma$  phases. The fitting parameters are described in text.

nant, compared with those of  $n=4m+1$ . On the other hand, the profile is fitted with the parameters  $p_3=0.03(1)$ ,  $p_4=0.85(1)$ ,  $p_5=0.08(1)$ , and  $p_6=0.04(1)$  in the  $\alpha$  phase, where the domain boundaries of  $n=4m+1$  are the majority.

The domain boundaries of  $n=4m-1$  in the  $\gamma$  phase are well explained by the structure model which was previously proposed in one of the STM works.<sup>4</sup> Figure 5(a) shows a schematic of the proposed structure. In this structure, a local structure reminiscent of the  $c(4\times 4)$  reconstruction<sup>22,23</sup> causes a separation of  $7a$  between neighboring  $2\times 4$  units. It seems reasonable that such an intermediate state appears in the transition from the  $2\times 4$  to the  $c(4\times 4)$  structure. A mixture of  $\beta 2-(2\times 4)$  and  $c(4\times 4)$  has been suggested also by combination of RHEED and RDS.<sup>3</sup> The disorder of  $4\times$  pe-

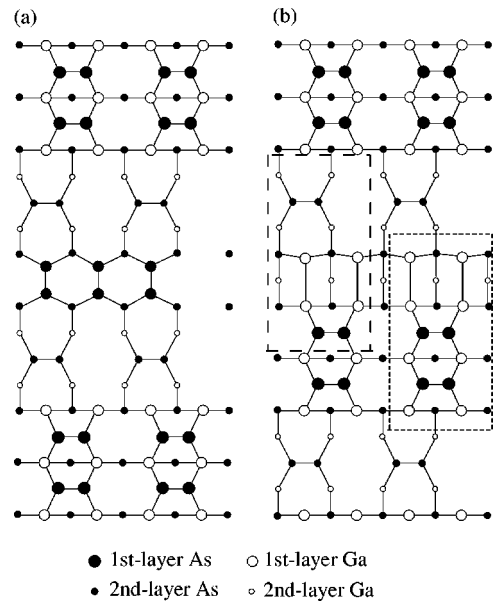


FIG. 5. Structure models of the domain boundaries between the neighboring  $\beta 2-(2\times 4)$  units for (a) the  $\gamma$  and (b) the  $\alpha$  phases. The model (a) for the  $\gamma$  phase was originally proposed by Hashizume *et al.*<sup>4</sup>

riodicity in the  $[110]$  direction has been observed also by a STM work on As desorption from the  $c(4\times 4)$  surface in vacuum.<sup>24</sup>

For the  $\alpha$  phase, the STM images showed the separations of  $3a$  and  $5a$  between the neighboring  $2\times 4$  units.<sup>4</sup> In these STM images, the fraction of  $3a$  was larger than that of  $5a$ , which disagrees with our result. We ascribe this discrepancy to the sample investigated. The STM observation was carried out at room temperature for the quenched samples. To verify the effect of quenching, we measured the x-ray-diffraction profiles after cooling the sample from  $610^\circ\text{C}$  to  $300^\circ\text{C}$  at a rate of  $10^\circ\text{C/s}$ . As a result of this treatment, the x-ray-diffraction peaks occurred at  $K=1.25$ ,  $K=0.75$ , and  $K=0.50$ , whereas they were as broad as in the  $\alpha$  phase. It was thus found that the characters at high temperature could be lost while the sample was being cooled. More recent STM work has revealed that the surface in the  $\alpha$  phase is covered with spontaneously formed two-dimensional islands.<sup>17,18</sup> These islands result in a lateral antiphase of  $a/2$  in the  $[110]$  and  $[1\bar{1}0]$  directions as well as step formation in the surface normal direction. However, the peak shift observed in the x-ray-diffraction profile cannot be accounted for by the existence of these islands. To reproduce the peak shift, therefore, the separation of  $5a$  between  $2\times 4$  domains is necessary apart from the island formation.

To interpret the separation of  $5a$  in the  $\alpha$  phase, we propose a structure shown in Fig. 5(b). This structure model is obtained simply by displacing the  $2\times 4$  unit by  $a$  in the  $[110]$  direction. Interestingly, the local structure surrounded by the dotted line in Fig. 5(b) is the structure that is referred to as  $\alpha$ - $(2\times 4)$ .<sup>1</sup> The STM images of the GaAs(001)- $2\times 4$  surface assigned to this structure are found in the literature.<sup>4,6,15,25</sup> Moreover, the area surrounded by the dashed line corresponds to the  $\alpha 2$ - $(2\times 4)$  structure which has been observed

on the InAs(001) surface by STM.<sup>26</sup> A recent theoretical calculation of surface energy has shown that the  $\alpha 2$ - $(2\times 4)$  structure is stable in an extremely narrow range of the As chemical potential between the ranges corresponding to the As-rich ( $2\times 4$ ) and the Ga-rich ( $4\times 2$ ) structures.<sup>27</sup> According to this calculation, the  $\alpha$ - $(2\times 4)$  structure is a metastable structure whose surface energy is higher than that of the  $\alpha 2$  structure by  $\sim 2\text{ meV}/\text{\AA}^2$ . Thus, it is not surprising that the  $\alpha$  or  $\alpha 2$  structures appear only at the domain boundaries without forming a single phase of these structures.

A more careful inspection of Fig. 2 reveals that the peak intensity at  $K=0.75$  significantly decreases in the  $\alpha$  phase, compared with the other peaks at  $K=1.25$  and  $K=0.5$ . This change in intensity can be accounted for by the partial missing of the topmost As dimers in the  $2\times 4$  unit cell. Besides, the antiphase domain boundaries may cause distortion of the adjacent  $2\times 4$  unit cells in both  $\alpha$  and  $\gamma$  phases. As a result, the scattering factor  $f$  of the  $2\times 4$  unit cells differs from the intrinsic one. The change of the scattering factor is not taken into consideration in the one-dimensional model employed in this paper. Nevertheless, the calculation agrees well with the observed profile. This is because the diffraction profile results from the discontinuity of the phase rather than the local structure as far as the peak position and width are concerned.

In conclusion, we investigated the  $\alpha$ ,  $\beta$ , and  $\gamma$  phases of the GaAs(001)- $2\times 4$  surface under conditions where MBE growth is actually performed. The fractional-order x-ray-diffraction peaks shift in the direction characteristic to the  $\alpha$  and  $\gamma$  phases. This peak shift is explained by the antiphase domain boundaries between the  $2\times 4$  units. We proposed structural models of the domain boundaries, which are consistent with the existing STM observations and first-principles calculations.

- 
- <sup>1</sup>H.H. Farrell and C.J. Palmstr n, J. Vac. Sci. Technol. B **8**, 903 (1990).  
<sup>2</sup>I. Kamiya, D.E. Aspnes, L.T. Florez, and J.P. Harbison, Phys. Rev. B **46**, 15 894 (1992).  
<sup>3</sup>A. Ohtake, M. Ozeki, T. Yasuda, and T. Hanada, Phys. Rev. B **65**, 165315 (2002).  
<sup>4</sup>T. Hashizume, Q.K. Xue, A. Ichimiya, and T. Sakurai, Phys. Rev. B **51**, 4200 (1995).  
<sup>5</sup>A.R. Avery, D.M. Holmes, J. Sudijono, T.S. Jones, and B.A. Joyce, Surf. Sci. **323**, 91 (1995).  
<sup>6</sup>L.D. Broekman, R.C.G. Leckey, J.D. Riley, A. Stampfl, B.F. Usher, and B.A. Sexton, Phys. Rev. B **51**, 17 795 (1995).  
<sup>7</sup>A. Ichimiya, Y. Nishikawa, and M. Uchiyama, Surf. Sci. **493**, 232 (2001).  
<sup>8</sup>Y. Garreau, M. Sauvage-Simkin, N. Jedrecy, R. Pinchaux, and M.B. Veron, Phys. Rev. B **54**, 17 638 (1996).  
<sup>9</sup>V.P. LaBella, H. Yang, D.W. Bullock, P.M. Thibado, P. Kratzer, and M. Scheffler, Phys. Rev. Lett. **83**, 2989 (1999).  
<sup>10</sup>D.J. Chadi, J. Vac. Sci. Technol. A **5**, 834 (1987).  
<sup>11</sup>J.E. Northrup and S. Froyen, Phys. Rev. B **50**, 2015 (1994).  
<sup>12</sup>S.B. Zhang and A. Zunger, Phys. Rev. B **53**, 1343 (1996).  
<sup>13</sup>W.G. Schmidt and F. Bechstedt, Surf. Sci. **360**, L473 (1996).  
<sup>14</sup>M.D. Pashley, K.W. Habernern, W. Friday, J.M. Woodall, and P.D. Kirchner, Phys. Rev. Lett. **60**, 2176 (1988).  
<sup>15</sup>J. Zhou, Q. Xue, H. Chaya, T. Hashizume, and T. Sakurai, Appl. Phys. Lett. **64**, 583 (1994).  
<sup>16</sup>A.R. Avery, C.M. Goringe, D.M. Holmes, J.L. Sudijono, and T.S. Jones, Phys. Rev. Lett. **76**, 3344 (1996).  
<sup>17</sup>V.P. LaBella, D.W. Bullock, M. Anser, Z. Ding, C. Emery, L. Bellaiche, and P.M. Thibado, Phys. Rev. Lett. **84**, 4152 (2000).  
<sup>18</sup>V.P. LaBella, D.W. Bullock, C. Emery, Z. Ding, and P.M. Thibado, Appl. Phys. Lett. **79**, 3065 (2001).  
<sup>19</sup>K. Kanisawa and H. Yamaguchi, Phys. Rev. B **56**, 12 080 (1997).  
<sup>20</sup>G.R. Bell, J.G. Belk, C.F. McConville, and T.S. Jones, Phys. Rev. B **59**, 2947 (1999).  
<sup>21</sup>M. Takahasi, Y. Yoneda, H. Inoue, N. Yamamoto, and J. Mizuki, Jpn. J. Appl. Phys., Part 1, **41**, 6247 (2002).  
<sup>22</sup>D.K. Biegelsen, R.D. Bringans, J.E. Northrup, and L.E. Swartz, Phys. Rev. B **41**, 5701 (1990).  
<sup>23</sup>M. Sauvage-Simkin, R. Pinchaux, J. Massies, P. Claverie, N. Je-

- drecy, J. Bonnet, and I.K. Robinson, Phys. Rev. Lett. **62**, 563 (1989).
- <sup>24</sup>M.J. Begarney, L. Li, C.H. Li, D.C. Law, Q. Fu, and R.F. Hicks, Phys. Rev. B **62**, 8092 (2000).
- <sup>25</sup>H. Xu, T. Hashizume, and T. Sakurai, Jpn. J. Appl. Phys., Part 1 **32**, 1511 (1993).
- <sup>26</sup>H. Yamaguchi and Y. Horikoshi, Phys. Rev. B **51**, 9836 (1995).
- <sup>27</sup>S.H. Lee, W. Moritz, and M. Sheffler, Phys. Rev. Lett. **85**, 3890 (2000).